Received: 22 October 2018 | Revised: 16 January 2019 | Accepted: 20 January 2019

DOI: 10.1111/cas.13949

ORIGINAL ARTICLE

WILEY Cancer Science

Frizzled 2-induced epithelial-mesenchymal transition correlates with vasculogenic mimicry, stemness, and Hippo signaling in hepatocellular carcinoma

Huohui Ou[1] | Zhanjun Chen[1] | Leyang Xiang[1] | Yinghao Fang[1] | Yuyan Xu[1] | Qin Liu[1] | Zhigang Hu[1] | Xianghong Li[1] | Yu Huang[2] | Dinghua Yang[1]

[1]Department of Hepatobiliary Surgery, Nanfang Hospital of Southern Medical University, Guangzhou, China

[2]Department of Laboratory Medicine, Nanfang Hospital of Southern Medical University, Guangzhou, China

Correspondence
Dinghua Yang, Department of Hepatobiliary Surgery, Nanfang Hospital of Southern Medical University, Guangzhou, China.
Email: dhyangyd@yahoo.com
and
Yu Huang, Department of Laboratory Medicine, Nanfang Hospital of Southern Medical University, Guangzhou, China.
Email: hy5810@yahoo.com

Funding information
Guangdong Provincial Science and Technology Projects, Grant/Award Number: 2017A020215132; National Natural Science Foundation of China, Grant/Award Number: 81872385

Prior observation has indicated that Frizzled 2 (FZD2)-induced epithelial-mesenchymal transition (EMT) could be a key step in metastasis and early recurrence of hepatocellular carcinoma (HCC). However, the mechanism underlying tumor development and progression due to aberrant FZD2 expression is poorly defined. Here, we provide evidence that FZD2 is a driver for EMT, cancer stem cell properties, and vasculogenic mimicry (VM) in HCC. We found that FZD2 was highly expressed in two cohorts of Chinese hepatitis B virus-related HCC patients, and that high FZD2 expression was associated with poor prognosis. Concerning the mechanism, gain- and loss-of-function experiments showed the oncogenic action of FZD2 in HCC cell proliferation, apoptosis, migration, and invasion. Further investigations in vitro and in vivo suggested that FZD2 promotes the EMT process, enhances stem-like properties, and confers VM capacity to HCC cells. Notably, integrative RNA sequencing analysis of FZD2-knockdown cells indicated the enrichment of Hippo signaling pathway. Taken together, our data suggest for the first time that FZD2 could promote clinically relevant EMT, $CD44^+$ stem-like properties, and the VM phenotype in HCC involving a potential Hippo signaling pathway-dependent mechanism, and should be considered as a promising therapeutic target for the treatment of HCC.

KEYWORDS
cancer stem cell, epithelial-mesenchymal transition, Frizzled 2, Hippo signaling pathway, vasculogenic mimicry

1 | INTRODUCTION

Hepatocellular carcinoma represents the sixth most common malignancy in the world and the third leading cause of cancer-related deaths worldwide, with particularly high morbidity in China due to the high incidence of HBV infection.[1] Although HCC is curable if detected early, most patients are diagnosed in the advanced stage and have an unfavorable outcome.[2] Tumor metastasis and recurrence

Abbreviations: CSC, cancer stem cell; DEG, differentially expressed gene; EMT, epithelial-mesenchymal transition; FDR, false discovery rate; FZD, Frizzled; HBV, hepatitis B virus; HCC, hepatocellular carcinoma; IHC, immunohistochemical; LATS1, large tumor suppressor kinase 1; MST1/2, mammalian sterile 20-like kinase 1/2; NC, negative control; PAS, periodic acid-Schiff; qRT-PCR, quantitative RT-PCR; RNA-Seq, RNA sequencing; SOX2, SRY-box 2; TAZ, Tafazzin; VM, vasculogenic mimicry; YAP, yes-associated protein.

Ou and Chen equally contributed to this study.

are the principal causes accounting for poor outcomes.[3] The clinical stage, based on the Barcelona Clinic Liver Cancer and TNM classification systems, is currently the most common prognostic factor at the time of diagnosis, but the molecular mechanism involved in HCC progression and metastasis is still unclear.[4] Thus, novel prognostic biomarkers and promising therapeutic targets that are associated with HCC progression and metastasis would be of great clinical significance.

Wnt proteins are a family of transcriptional genes that play pivotal roles in cell survival, migration, and invasion by coordinating with one or more of the FZD receptors.[5] Multiple studies have reported that the canonical Wnt/β-catenin signaling pathway is activated during EMT.[6-8] Among them, a study has revealed that FZD2 drives EMT and cell metastasis through a previously unrecognized, noncanonical pathway that involves molecules such as the tyrosine kinase (FYN) and STAT3.[9] Another study confirmed that FZD2 upregulation was significantly correlated with EMT status in HCC.[10]

Epithelial-mesenchymal transition has been associated with CSC properties and VM in several tumors.[11-13] Cancer stem cells are a small subgroup within tumors that are capable of self-renewal and maintain tumor-initiating capacity through differentiation into the heterogeneous nature of tumor cells that comprise the primary tumor. They also provide the possibility for cells that cause tumor recurrence and drug resistance. Increasing evidence indicates that VM, the formation of a vascular-like structure that mimics the embryonic vascular network pattern to support tumor tissue, is a critical step in tumor progression, invasion, and metastasis. Since the discovery of VM, research has been carried out on the molecular mechanism by which VM formation emerges, in an effort to identify valuable therapeutic targets. The noncanonical Wnt signaling pathway, which provides important clues to tumorigenesis, is implicated in both VM and CSCs,[14-16] and thus is of great concern. In this study, we found that FZD2 might be implicated in EMT-mediated metastasis and CSC maintenance, as well as VM through interacting with Hippo signaling, in HCC. Our study provides a plausible mechanism for HCC metastasis and early recurrence.

2 | MATERIALS AND METHODS

2.1 | Patients and tissue samples

Two independent cohorts, each consisting of 100 HCC patients with HCC, were enrolled in this study. Patient inclusive criteria were as follows: (a) pathologically diagnosed with HCC; (b) received radical resection in the Department of Hepatobiliary Surgery at Nanfang Hospital of Southern Medical University (Guangzhou, China) between 2010 and 2015; (c) without a history of any antitumor treatment; and (d) with complete medical record and follow-up data. In cohort 1, fresh HCC tissue samples and adjacent noncancerous tissues from 100 patients were used for qRT-PCR. In cohort 2, paraformaldehyde-fixed, paraffin-embedded tissues from 100 patients were used for IHC staining. This study was approved by the ethics committee of Nanfang Hospital of Southern Medical University. Patients' samples were collected after informed consent in accordance with the Declaration of Helsinki.

2.2 | Cell lines

Hepatocellular carcinoma cell lines SNU387, SNU449, and HepG2 were obtained from the ATCC (Manassas, VA, USA). The cells were cultured in RPMI-1640 (SNU387 and SNU449) or DMEM (HepG2) (Corning, Logan, UT, USA) supplemented with 10% FBS (Corning) at 37°C in a humidified 5% CO_2 incubator.

2.3 | Animals

Male BALB/c-nude mice (4-6 weeks old) were obtained from the Central Laboratory of Animal Science, Southern Medical University (Guangzhou, China) and were raised under specific pathogen-free conditions. Animal experiments were carried out in accordance with the Guide for the Care and Use of Laboratory Animals, which were approved by the Institutional Animal Care and Use Committee of Southern Medical University.

2.4 | Quantitative RT-PCR analysis

Total RNA was extracted using the RNAiso reagent (TaKaRa, Dalian, China). Quantitative PCR was carried out using the SYBR Premix Ex Taq kit (TaKaRa) following the manufacturer's instructions. Results were normalized to the expression levels of GAPDH. Primers sequences were as follows: FZD2 forward primer, 5′-TCC TCA AGG TGC CAT CCT ATC TC -3′ and reverse primer, 5′-TGG TGA CAG TGA AGA AGG TGG AAG-3′; and GAPDH forward primer, 5′- CAG GAG GCA TTG CTG ATG AT-3′ and reverse primer, 5′-GAA GGC TGG GGC TCA TTT-3′. The qRT-PCR assay results were analyzed by the $2^{-\Delta\Delta CT}$ method.[17]

2.5 | Immunohistochemistry staining

Immunohistochemistry staining was undertaken as described in our previous report.[18] The expression of FZD2 was examined by light microscopy by evaluating 1000 cells in 5 fields to obtain the percentage of positive cells, which was multiplied by staining intensity to produce a weighted score for each case. Cases with a weighted score of 0-3 were regarded negative and those with a score of 4-8 positive. Primary Abs are listed in Table S1.

2.6 | CD34/PAS double staining

To display the VM structures in HCC human samples and mouse xenografts, histological sections were IHC stained for CD34, then stained with PAS (cat. BA4080A; BASO, Zhuhai, China) following the manufacturer's instructions.

2.7 | Small interfering RNA transient transfection

For transient FZD2 silencing, SNU387 and SNU449 cells were transfected with siRNAs (GenePharma, Shanghai, China) in 6-well plates for 48 hours. The siRNA sequences were as follows: siRNA-1 (targeting 5′-TCT CAA CTG CTT TGC TCC CAT CAA T-3′), siRNA-2 (targeting 5′-GCC AGG TGG TCA TGC TCA ACT ACA A-3′), and NC (targeting 5′-TTC TCC GAA CGT GTC ACG TTT-3′).

2.8 | Lentiviral construction and cell transfection

The U6-sh-FZD2-UFC1-CMV-GFP lentiviral vector was purchased from Genechem (Shanghai, China) and was used to stably knock down FZD2 expression. A negative control lentiviral vector containing nonsilencing shRNA was used. SNU449 cells were infected with either of the lentiviral vectors at an MOI of 20. To generate clones stably overexpressing FZD2, HepG2 cells were infected at an MOI of 40 with a lentiviral vector harboring a full-length human FZD2 sequence or empty lentiviral vector control.

2.9 | Cell viability assay

Cells (1×10^3/well) were seeded in 96-well plates and cell viability was evaluated from 6 replicates with the CCK-8 (Dojindo Laboratories, Kumamoto, Japan) at 0, 24, 48, 72, and 96 hours after siRNA transfection.

2.10 | Flow cytometric analysis

For the apoptosis assay, cells (1×10^6) were stained with annexin V-APC (allophycocyanin) and DAPI (Apoptosis Detection Kit; KeyGEN, Nanjing, China) and analyzed with a flow cytometer (BD Biosciences, San Diego, CA, USA). To identify the $CD44^+$ subpopulation, cells were labeled with a phycoerythrin-conjugated anti-CD44 Ab (eBioscience, San Diego, CA, USA). Cells incubated without labeled Ab were used as NC. Cells were incubated with 5 μL Ab at room temperature for 30 minutes before detection on a flow cytometer. The data were analyzed using FlowJo software (Tree Star, Ashland, OR, USA).

2.11 | Migration and invasion assays

For migration assay, cells (5×10^4) were resuspended in serum-free medium and then cultured in the upper chamber of a Transwell insert (8-μm pore size; Millipore, Billerica, MA, USA). For invasion assay, cells (5×10^4) were resuspended in serum-free medium and then cultured in the upper chamber of an insert coated with 100% Matrigel. Complete medium with 10% FBS was added to the lower chamber. After incubation for 24-48 hours, the cells that had migrated or invaded through the membrane were stained with 0.1% crystal violet and photographed under an inverted microscope.

2.12 | Western blot analysis

Cells were lysed with RIPA buffer (Beyotime, Jiangsu, China) containing 1 mM PMSF. Equivalent total protein (30 μg) was separated by 10% SDS-PAGE. The separated proteins were transferred to a PVDF membrane. The membrane was trimmed and blocked with 5% BSA for 1 hour, and probed with primary Abs (Table S1) overnight at 4°C. Then the membranes were incubated with corresponding HRP-conjugated secondary Abs diluted in blocking buffer for 1 hour at 37°C. Protein immunocomplexes were visualized by an enhanced chemiluminescence detection agent (Beyotime). The membrane was scanned by Quantity One (Bio-Rad, Hercules, CA, USA). To evaluate the nuclear fractions of YAP, a nuclear-cytosol extraction kit (FDbio Science, Hangzhou, China) was used. Histone H3 was used as a loading control for nuclear protein.

2.13 | Three-dimensional tube formation assay

A 3D culture was used to assess the ability of tumor cells to form a VM structure. Cells (2×10^4) were resuspended in a 200-μL mixture of equal volumes of serum-free DMEM or RPMI-1640 medium, and then placed into 60% Matrigel-coated 96-well plates. After incubation for 4 hours at 37°C, the branch points of the formed tubes, which represented the degree of VM formation, were quantitated under an inverted microscope.

2.14 | Tumorigenicity assay

To establish an s.c. xenograft model, 10 male BALB/c nude mice at 5-6 weeks of age were used. Stable knockdown and overexpressing HCC cell lines were injected s.c. into the posterior-lateral side of each mouse. Tumor growth was recorded every 5 days till 30 days. The length (L) and width (W) of the tumor was measured and the tumor volume (V) was calculated with the formula: $V = L \times W^2 \times \pi/6$. Tumor samples were fixed in paraformaldehyde and embedded in paraffin for IHC staining.

2.15 | RNA sequencing analysis

Total RNA for RNA-Seq was isolated from SNU449 cells infected with either of the lentiviral vectors encoding specific shRNA sequences or the NC vector. Total RNA was quantified and integrity was measured on a BioAnalyzer 2100 (Agilent, Santa Clara, CA, USA). Oligo(dT) magnetic beads were used to select mRNA with polyA tail and the target RNA was obtained after purification. The RNA was fragmented and reverse-transcribed into double-stranded cDNA using N6 random primer. The double-stranded cRNA was processed for end repair and was then ligated with adaptor and amplified by PCR. The PCR products were denatured by heating and the single-stranded cDNA was cyclized using splint oligo and DNA ligase. The cDNA library was sequenced by BGISEQ-500 (BGI, Shenzhen, China). After primary sequencing data passed quality control, the raw reads were filtered to obtain clean reads, which were aligned

to the reference genome using HISAT and to reference gene sequences using Bowtie2. Gene expression was quantified by RSEM. Differentially expressed genes between FZD2 shRNA-transfected versus control cells were screened using the Poisson distribution method. We used FDR ≤ .001 and $|\text{Log}_2\text{Ratio}| \geq 1$ as thresholds to judge the significance of gene expression difference. Differentially expressed genes were subjected to Kyoto Encyclopedia of Genes and Genomes pathway enrichment analysis.

2.16 | Statistical analysis

All experiments were carried out in triplicate and data are presented as the mean ± standard deviation. Means were compared by Student's *t* test or one-way ANOVA with either SPSS 19.0 software (SPSS, Chicago, IL, USA) or GraphPad Prism 5 (GraphPad Software, La Jolla, CA, USA). Survival curves were calculated using the Kaplan-Meier method. Differences were considered statistically significant when $P < .05$.

3 | RESULTS

3.1 | Upregulation of FZD2 in HCC tissues predicts tumor progression and poor survival

We evaluated FZD2 expression in HCC tissues from 2 cohorts of patients with HCC. In cohort 1, we analyzed FZD2 expression by

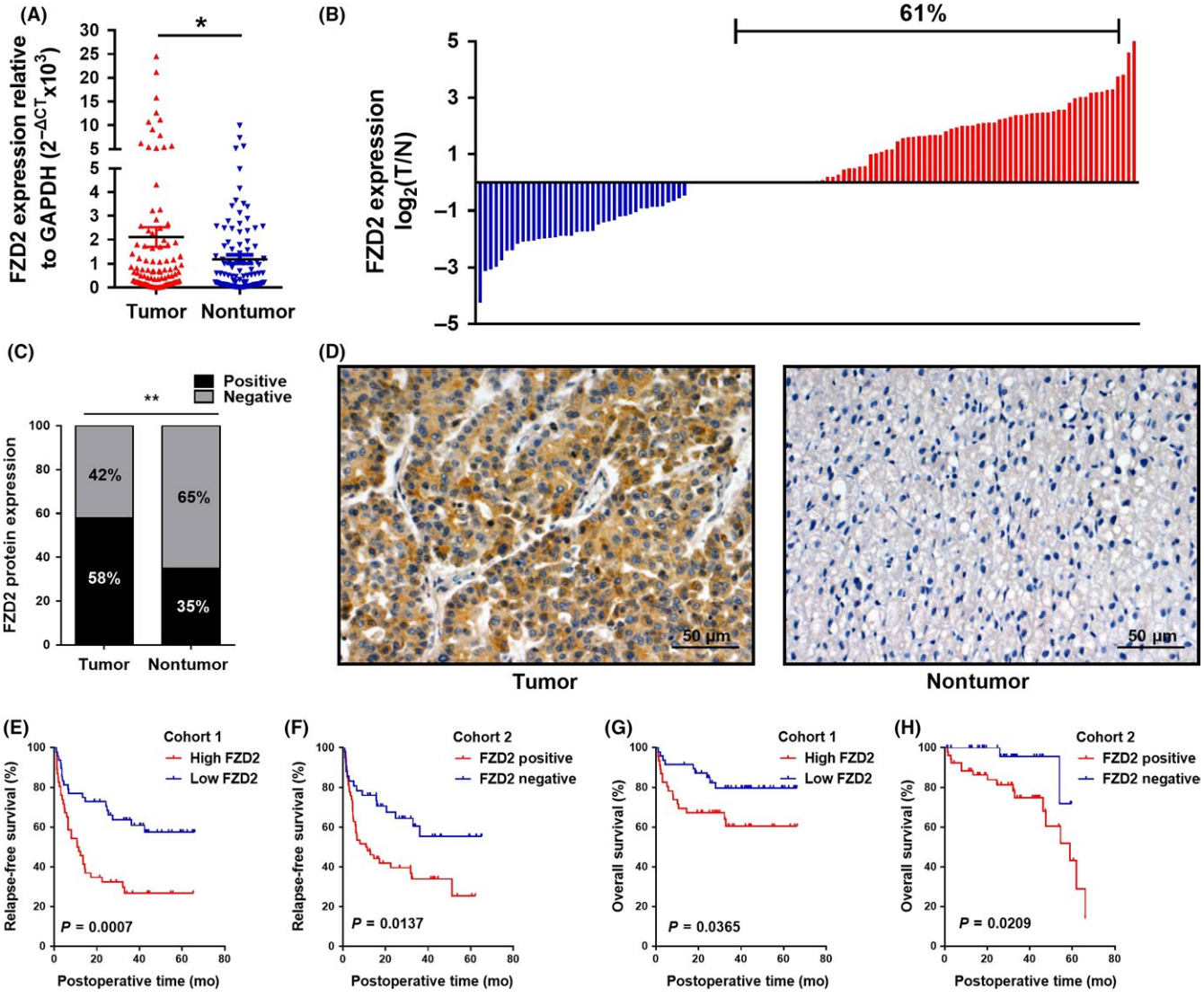

FIGURE 1 Frizzled 2 (FZD2) is overexpressed in hepatocellular carcinoma (HCC) tissues and predicts poor survival for patients with HCC. A, FZD2 mRNA expression was analyzed by quantitative RT-PCR in HCC tissues and adjacent nontumor tissues (cohort 1, n = 100). *$P < .05$. B, FZD2 was upregulated in 61/100 (61%) of HCC cases. Data are presented as the $\log_2$ ratio of the FZD2 mRNA level in HCC tissues versus that in adjacent nontumorous tissues. C, FZD2 protein expression was detected by immunohistochemical staining (cohort 2, n = 100). D, Representative images of immunohistochemical staining for FZD2 in HCC tissues. E,F, Kaplan-Meier analysis of relapse-free survival in HCC patients from cohort 1 ($P = .0007$) and cohort 2 ($P = .0137$). Differences were assessed by log-rank test. G,H, Kaplan-Meier analysis of overall survival in HCC patients from cohort 1 ($P = .0365$) and cohort 2 ($P = .0209$). Differences were assessed by log-rank test. **$P < .01$

TABLE 1 Clinicopathologic characteristics of 100 patients with hepatocellular carcinoma: fresh tissue samples from cohort 1 assessed by quantitative RT-PCR

Feature	N	FZD2 mRNA expression level		*P* value[b]
		High expression	Low expression	
Sex				
Male	90	46	44	.505
Female	10	6	4	
Age, y				
<60	85	44	41	.401
≥60	15	6	9	
AFP level, μg/L				
<400	59	28	31	.542
≥400	41	22	19	
Cirrhosis				
Yes	72	40	32	.075
No	28	10	18	
Tumor capsule				
Present	74	35	39	.362
Absent	26	15	11	
Tumor size, cm				
<5	53	21	32	**.028**
≥5	47	29	18	
Tumor number				
Solitary	79	39	40	**.028**
Multiple	21	10	11	
Differentiation				
Well	13	2	11	**.013**
Moderate	61	31	30	
Poor	26	17	9	
PVTT				
Present	20	14	6	**.046**
Absent	80	36	44	
MVI				
Present	33	23	10	**.006**
Absent	67	27	40	
TNM stage				
I+II	46	18	28	**.045**
III+IV	54	32	22	
BCLC stage				
A	43	18	28	**.032**
B	9	32	22	
C	48	30	18	
Metastasis				
Yes	51	31	20	**.028**
No	49	19	30	
Early recurrence[a]				
Yes	35	24	11	**.003**
No	59	22	37	

[a]Defined as relapse-free time <12 months, and 6 cases were lost to follow-up.
[b]Values in bold indicated statistically significant.
AFP, α-fetoprotein; BCLC, Barcelona Clinic Liver Cancer; MVI, microvascular invasion; PVTT, portal vein tumor thrombus.

TABLE 2 Clinicopathologic characteristics of 100 patients with hepatocellular carcinoma: paraformaldehyde-fixed, paraffin-embedded tissues from cohort 2 assessed by immunohistochemical staining

Feature	N	FZD2 protein expression level		*P* value[b]
		High expression	Low expression	
Sex				
Male	82	46	36	0.411
Female	18	12	6	
Age, year				
<60	84	50	34	0.479
≥60	16	8	8	
AFP level, μg/L				
<400	66	35	31	0.161
≥400	34	23	11	
Cirrhosis				
Yes	60	41	19	**0.010**
No	40	17	23	
Tumor capsule				
Present	42	23	19	0.577
Absent	58	35	23	
Tumor size, cm				
<5	50	21	29	**0.001**
≥5	50	31	13	
Tumor number				
Solitary	84	47	37	0.342
Multiple	16	11	5	
Differentiation				
Well	13	6	8	**0.005**
Moderate	61	37	33	
Poor	26	15	1	
PVTT				
Present	47	40	7	**0.000**
Absent	53	18	35	
MVI				
Present	60	41	19	**0.010**
Absent	40	17	23	
TNM stage				
I+II	64	32	32	**0.031**
III+IV	36	26	10	
BCLC stage				
A	60	27	33	**0.005**
B	10	8	2	
C	30	23	7	
Metastasis				
Yes	48	36	12	**0.001**
No	52	22	30	
Early recurrence[a]				
Yes	39	28	11	**0.009**
No	56	25	31	

[a]Defined as relapse-free time <12 months, and 5 cases were lost to follow-up.
[b]Values in bold indicated statistically significant.
AFP, α-fetoprotein; BCLC, Barcelona Clinic Liver Cancer; MVI, microvascular invasion; PVTT, portal vein tumor thrombus.

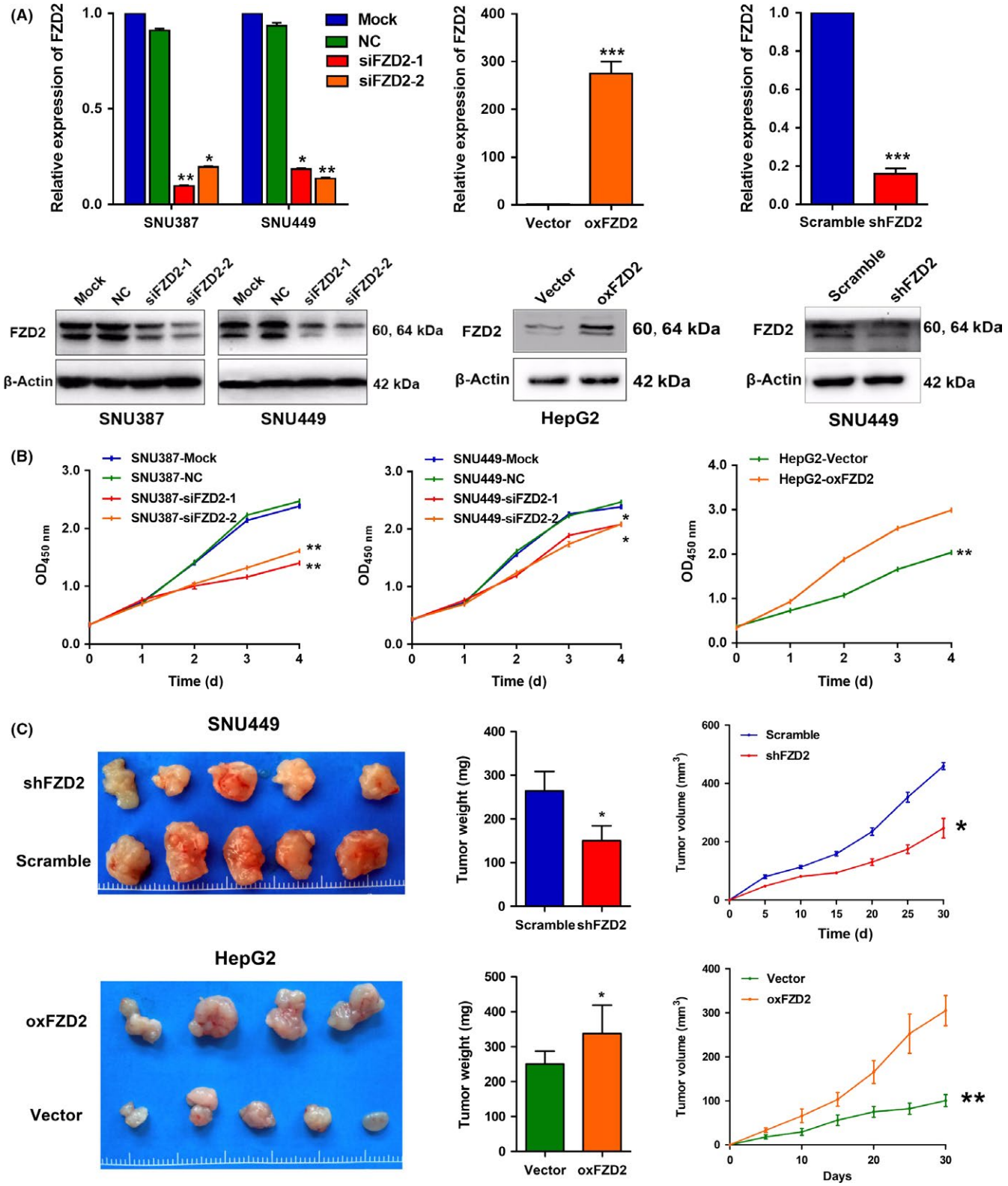

FIGURE 2 Frizzled 2 (FZD2) promotes hepatocellular carcinoma cell proliferation in vitro and in vivo. A, Knockdown of FZD2 in SNU387 and SNU449 cells and overexpression of FZD2 were confirmed by quantitative RT-PCR and western blot analysis. B, Cell growth was determined by CCK-8 assay. C, Tumor size (left panels), weight (middle panels), and volume (right panels) of xenografts harvested at 30 days after s.c. injection of FZD2-knockdown SNU449 cells and FZD2-overexpressing HepG2 cells in nude mice. *$P < .05$, **$P < .01$. NC, negative control

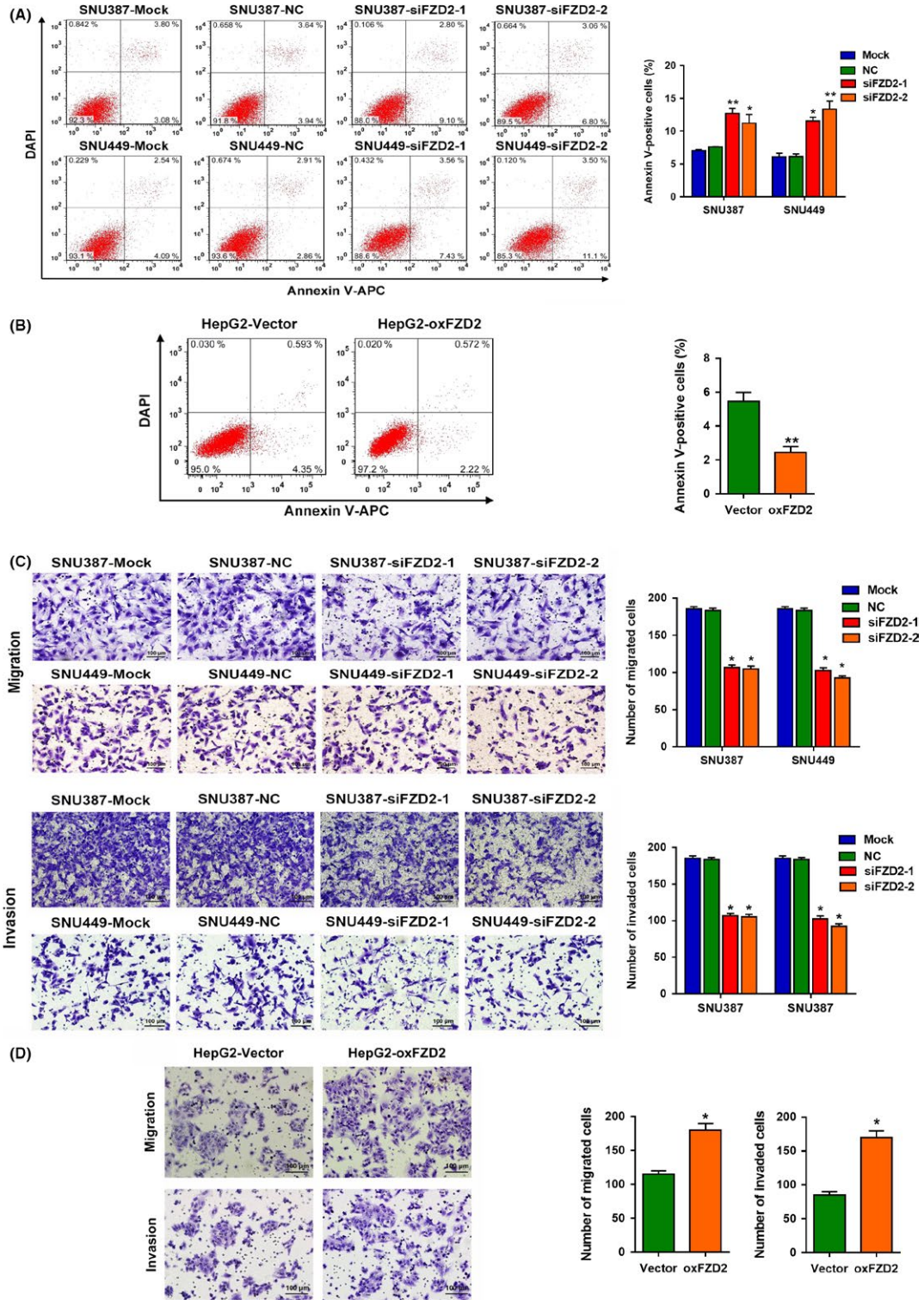

FIGURE 3 Frizzled 2 (FZD2) inhibits hepatocellular carcinoma cell apoptosis and enhances hepatocellular carcinoma cell migration and invasion. A,B, Percentages of apoptotic cells with annexin V staining were analyzed by flow cytometry. C,D, Numbers of migrated and invaded cells were tested by Transwell assays. **P* < .05, ***P* < .01. NC, negative control

qRT-PCR in 100 pairs of HCC/nontumor tissues, and we found that the FZD2 mRNA level was significantly higher in HCC tissues than in adjacent nontumor tissues ($P = .0411$; Figure 1A,B). The elevated FZD2 expression was confirmed by IHC staining of an additional 100 pairs of paraffin-embedded HCC/noncancerous specimens from cohort 2. The results showed the upregulation of FZD2 in HCC and suggested that FZD2 is localized in the cytoplasm of cancer cells ($P < .01$; Figure 1C,D).

We then analyzed the association between FZD2 and clinicopathologic parameters in HCC patients. Statistical analysis indicated a strong correlation between FZD2 expression and tumor size ($P = .028$ and $P = .010$, in cohorts 1 and 2, respectively), differentiation ($P = .013$ and $P = .005$), portal vein tumor thrombus ($P = .046$ and $P = .000$), microvascular invasion ($P = .006$ and .010), TNM stage ($P = .045$ and $P = .031$), Barcelona Clinic Liver Cancer stage ($P = .032$ and $P = .005$), metastasis ($P = .028$ and $P = .001$), and early recurrence ($P = .003$ and $P = .009$) (Tables 1 and 2). Kaplan-Meier analysis suggested a positive correlation between cancerous FZD2 expression and significantly reduced relapse-free survival and overall survival (all $P < .05$; Figure 1E-H).

3.2 | Frizzled 2 promotes cell proliferation, inhibits cell apoptosis, and enhances cell migration and invasion in HCC

We explored the potential role of FZD2 in the development and progression of HCC. To this end, we transiently silenced FZD2 expression in SNU387 and SNU449 cell lines for in vitro loss-of-function experiments; we also established a HepG2 cell line stably overexpressing FZD2 and a SNU449 cell line with stable FZD2 depletion for in vivo experiments. Silencing and overexpression were confirmed by qRT-PCR and western blot analysis (Figure 2A). A CCK-8 assay revealed that FZD2 depletion inhibited the proliferative capacity of SNU387 and SNU449 cells compared with that of control cells.

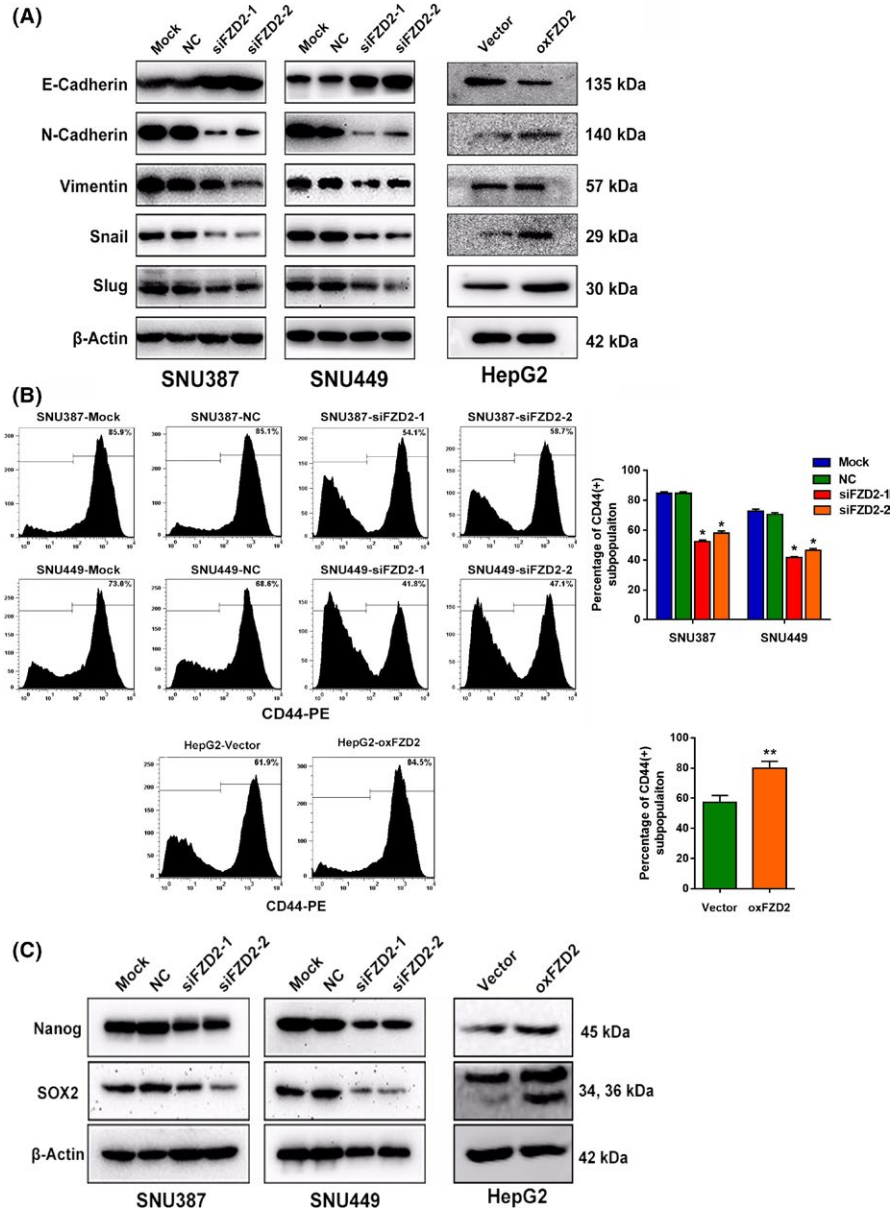

FIGURE 4 Frizzled 2 (FZD2) induces epithelial-mesenchymal transition and maintains cancer stem cell properties of hepatocellular carcinoma cells. A, Epithelial-mesenchymal transition-related proteins E-cadherin, N-cadherin, Vimentin, Snail, and Slug were detected by western blot analysis. B, Percentage of $CD44^+$ cells were analyzed by flow cytometry. C, Nanog and SOX2 protein were detected by western blot analyses. $^*P < .05$, $^{**}P < .01$. NC, negative control

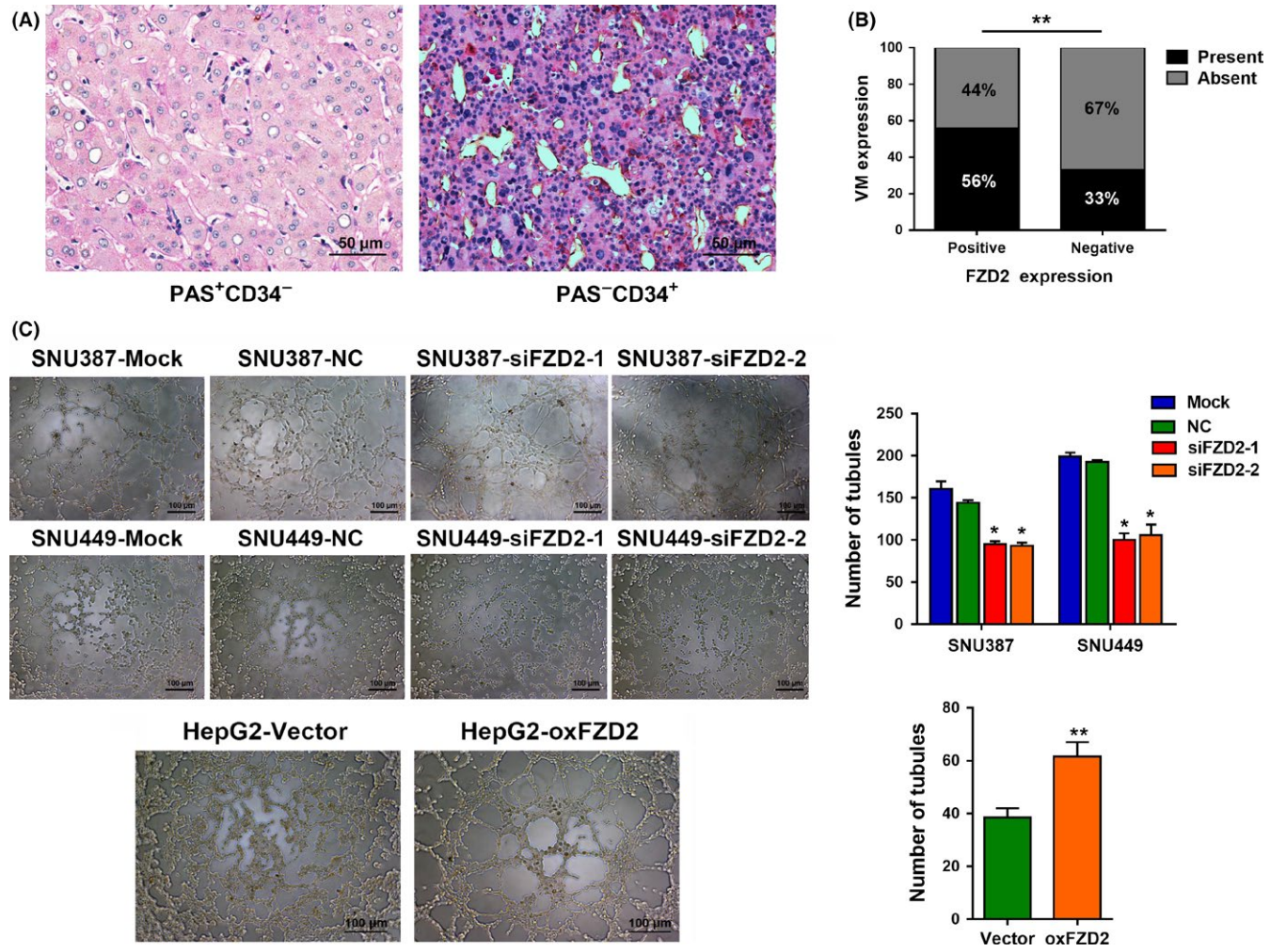

FIGURE 5 Frizzled 2 (FZD2) confers hepatocellular carcinoma (HCC) cells with vasculogenic mimicry (VM) ability. A, Representative images of VM with H&E staining in HCC tissues from cohort 2. The VM channel was periodic acid-Schiff (PAS)$^+$, but it did not express CD34. Endothelium-dependent vessel was CD34$^+$. B, FZD2 expression is positively correlated with the existence of a VM structure in HCC tissues from cohort 2. C, Representative images of tube formation by FZD2-knockdown SNU387 and SNU449 cells and FZD2-overexpressing HepG2 cells after 3D culture; numbers of tube-like structures are shown. *P < .05, **P < .01. NC, negative control

Overexpression of FZD2 dramatically enhanced the proliferative capacity of HepG2 cells (Figure 2B). The growth inhibition effect was confirmed in vivo by a tumor growth assay. Xenograft tumors grown from FZD2-knockdown SNU449 cells had lower weights and volumes than tumors grown from control cells. Tumors derived from FZD2-overexpressing cells were larger than control ones (Figure 2B). These results indicated that FZD2 might facilitate HCC cell proliferation both in vitro and in vivo.

To determine whether FZD2 might be critical for tumor survival, we evaluated apoptosis by FACS analysis in HCC cells stained with annexin V. We found that FZD2-knockdown SNU387 and SNU449 cells had a significantly higher proportion of annexin V-positive cells than cells transfected with NC-siRNA, whereas a significant decrease in annexin V-positive cells was observed in FZD2-overexpressing HepG2 cells (Figure 3A,B).

To determine the role of FZD2 in tumor metastasis, Transwell assays were carried out. Knockdown of FZD2 markedly decreased the migratory and invasion capacities of SNU387 and SNU449 cells (Figure 3C). Furthermore, FZD2-overexpressing HepG2 cells showed stronger migratory and invasive abilities than the control group (Figure 3D). These results indicated a positive correlation between FZD2 expression and aggression of HCC.

3.3 | Frizzled 2 drives EMT in HCC

Epithelial-mesenchymal transition plays a vital role in cancer metastasis and progression. The loss of E-cadherin expression and the gain of N-cadherin and Vimentin expression represents the molecular event of EMT. Therefore, we determined the levels of these EMT markers in FZD2-knockdown and -overexpressing cells. Knockdown of FZD2 induced expression of E-cadherin and suppressed that of N-cadherin, Vimentin, Snail, and Slug, whereas overexpression of FZD2 attenuated E-cadherin expression and promoted N-cadherin, vimentin, Snail, and Slug expression (Figure 4A).

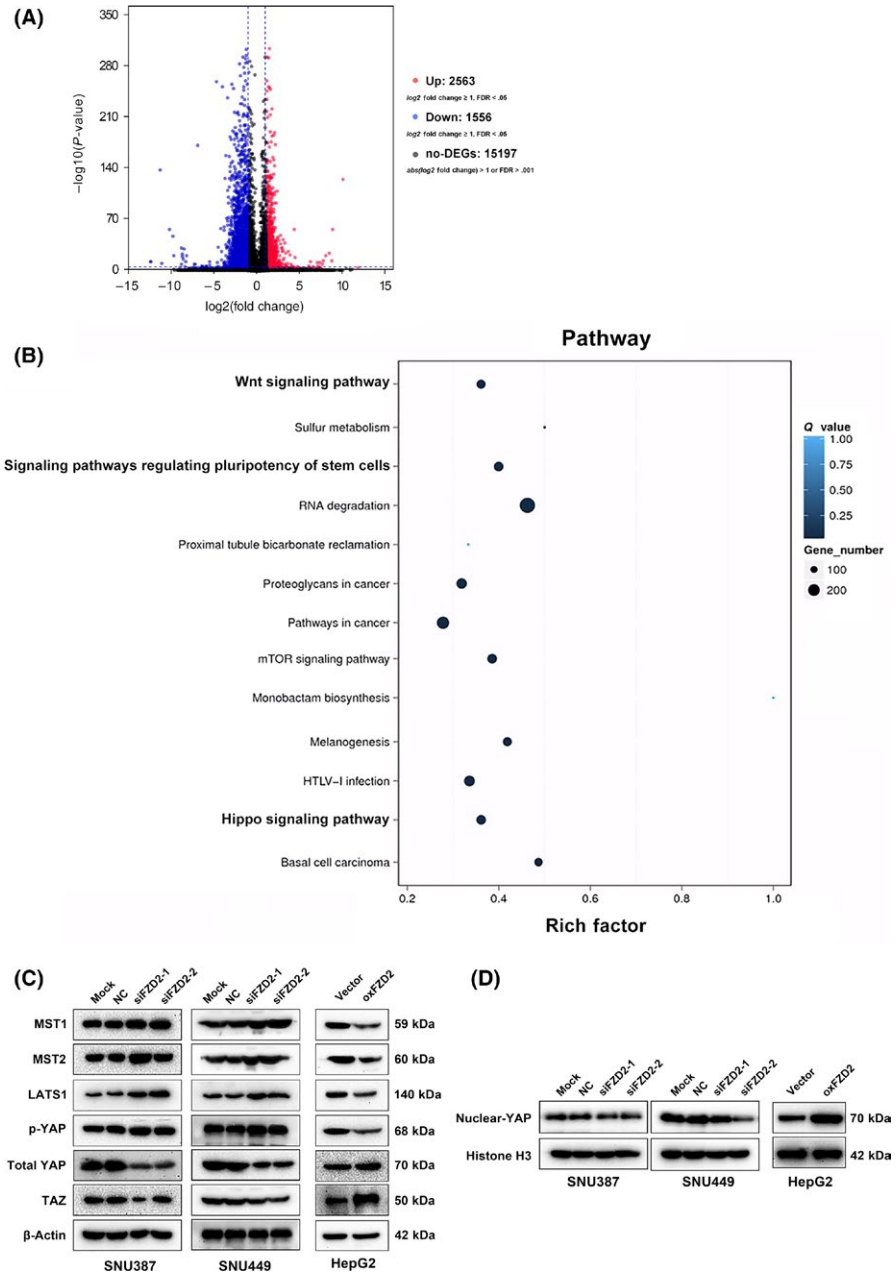

FIGURE 6 RNA sequencing reveals that the Hippo signaling pathway is enriched following stable silencing of Frizzled 2 (FZD2) in SNU449 cells. A, Volcano plot of differentially expressed genes (DEGs). Each dot represents a DEG. Significant DEGs (false discover rate [FDR] ≤ .001 and |Log2Ratio| ≥1) are indicated in red and nonsignificant DEGs in black. B, Kyoto Encyclopedia of Genes and Genomes pathway enrichment analysis of DEGs. C, Mammalian sterile 20-like kinase (MST)1, MST2, large tumor suppressor kinase (LATS)1, phosphorylated Yes-associated protein (p-YAP), total YAP, and Tafazzin (TAZ) were detected by western blot analysis. D, Nuclear YAP was detected by western blot analysis. NC, negative control

Similar effects were observed by IHC staining of xenograft tumor tissues (Figure S1).

3.4 | Frizzled 2 increases stem-like properties of HCC

The recent discovery that CSCs emerge, in part, as a result of EMT has provided a new understanding of the regulatory mechanisms in CSCs.[19] To identify the stemness phenotype, we assessed the expression of the CSC-specific surface marker CD44. Flow cytometric analysis showed that knockdown of FZD2 in SNU387 and SNU449 cells resulted in a significant reduction in the $CD44^+$ subpopulation, and overexpression of FZD2 promoted the $CD44^+$ subpopulations in HepG2 cells (Figure 4B). In addition, we examined the expression of 2 transcription factors that are characteristic of pluripotent cells: Nanog and SOX2. Following knockdown of FZD2 in SNU387 and SNU449 cells, Nanog and SOX2 were downregulated (Figure 4C). Overexpression of FZD2

in HepG2 cells brought about an opposite effect (Figure 4C). The effect of FZD2 on Nanog and SOX2 expression was further supported by IHC staining in xenograft tumor tissues (Figure S1). These findings supported that FZD2 regulated the CSCs feature of HCC cells.

3.5 | Frizzled 2 promotes VM formation of HCC cells

With the increasing knowledge about CSC phenotypes and functions, the CSCs concept has been applied to VM, which has also been recently observed in HCC.[20] To elucidate the effect of FZD2 on VM, we evaluated the relationship between FZD2 expression and VM structures in clinical samples. Vasculogenic mimicry structures were visualized by CD34/PAS double staining and were identified as vascular-like channels that were lined by tumor cells, displayed positive staining for PAS but negative staining for CD34 (PAS^+CD34^-), and possibly contained erythrocytes (Figure 5A). The presence of a VM structure in an HCC section was designated as VM+, and cases without a VM structure in a whole HCC section were considered VM− cases. There were more VM+ cases in the $FZD2^+$ group than in the $FZD2^-$ group ($P < .01$; Figure 5B). These data suggested a positive correlation between FZD2 and VM in clinical specimens. To gain further insight into the correlation between FZD2 expression and VM, a 3D tube formation assay was carried out. As shown in Figure 5C, both SNU387 and SNU449 cells could form typical channels in the in vitro 3D culture model, but the number of branch points decreased when the cells were transfected with FZD2 siRNA. Moreover, compared with the control group, HepG2 cells overexpressing FZD2 formed more tube-like structures, and the inner walls of these pipes were smoother. Vasculogenic mimicry structures were also evaluated in the xenograft tumor tissues. In agreement with the results of 3D culture, $PAS^+/CD34^-$ structures were decreased in the FZD2-depleted cells and were increased in the FZD2-overexpressing cells as compared with their corresponding controls (Figure S2). Collectively, the in vitro and in vivo data indicated that FZD2 promotes VM of HCC cells.

3.6 | Frizzled 2 is a regulator of HCC cell invasion and metastasis by activating the Hippo-YAP pathway

To determine the gene networks underlying the biological consequences of FZD2 knockdown, RNA-Seq analysis was carried out. In SNU449 cells transfected with FZD2 shRNA, a total of 4119 genes were differentially expressed (2563 upregulated and 1556 downregulated genes, with $|Log_2Ratio| \geq 1$ and an adjusted P value [FDR Q value] < .001; Figure 6A). Kyoto Encyclopedia of Genes and Genomes pathway enrichment analysis of DEGs revealed that *FZD2* gene networks were closely related to the Hippo pathway (Figure 6B). To validate whether the Hippo pathway is involved in FZD2 dysregulation, YAP activity and TAZ levels were evaluated. Yes-associated protein activity is determined by its phosphorylation status and cellular localization. Following phosphorylation, YAP is translocated from the nucleus to the cytoplasm for proteasome-mediated degradation.[19,20] We also measured the cytosolic kinases upstream of YAP including LATS1, which phosphorylates and inhibits YAP, and MST1/2, which phosphorylates and activates LATS1, and the phosphorylation level of YAP. As shown in Figure 6C, FZD2 knockdown significantly increased the expression levels of LATS1, MST1/2, and the phosphorylation level of YAP ($p\text{-}YAP^{ser127}$) in SNU387 and SNU449 cells. In contrast, FZD2 overexpression suppressed these proteins in HepG2 cells. Furthermore, FZD2 knockdown resulted in a marked loss of nuclear YAP in SNU387 and SNU449 cells, whereas an increase in nuclear YAP was observed in HepG2 cells overexpressing FZD2 (Figure 6D). The expression levels of total YAP and TAZ were consistent with the level of nuclear YAP (Figure 6C). These data indicated that the tumorigenic effects of FZD2 in HCC might depend on the activity of YAP involved in the Hippo signaling pathway.

4 | DISCUSSION

In a previous study, Gujral et al[9] reported that FZD2 is upregulated in poorly differentiated mesenchymal cancers, that FZD2 regulates EMT and migration, and that use of a blocking Ab against FZD2 was sufficient to abrogate metastases in a xenograft model. Similarly, Asano et al reported that mRNA levels of FZD2 were prognostic in a cohort of 100 patients and were associated with the EMT phenotype. Our study extends their findings based on 2 cohorts of HCC patients with HBV infection, and provides a full understanding of the clinical implications at both the mRNA and protein levels. We found that FZD2 was frequently upregulated in HCC tissues relative to corresponding adjacent nontumor tissues at both the transcriptional and the translational level. High expression of FZD2 was associated with tumor progression and poor outcome of patients with HCC and should be considered as a promising prognostic biomarker for this disease. We also confirmed the importance of FZD2-mediated EMT on more malignant biological properties of HCC including CD44 phenotypic stemness and VM formation, reinforcing the view that EMT is a fundamental event.

Recent studies show that EMT can confer tumor cells with stem cell-like characteristics.[21,22] In prostate cancer, recent evidence suggested that transforming growth factor-β-induced EMT was mechanistically linked to the formation of highly tumorigenic prostate cancer stem cells with a mesenchymal phenotype, and involved in the upregulation of Snail and Nanog.[23] Enhanced self-renewal, tumor-initiating capacity, and chemoresistance have been attributed to subsets of cancer cells with high CD44 expression in HCC.[24] Studies in breast cancer indicated that EMT might promote conversion of a subset of cancer cells defined by low CD44 expression to those with high CD44 expression.[19,21] An effort has been made in our study to bridge CD44 stem-like subsets with aberrant FZD2 levels by FACS analysis. Further experiments suggested that FZD2 might confer HCC cells with CD44 stem-like properties by regulating

the activity of Nanog and SOX. Interestingly, our results in RNA-Seq also revealed that *FZD2* gene networks were significantly associated with signaling pathways regulating the pluripotency of stem cells. In all, we can assume that the action of FZD2-mediated EMT could be involved in the acquisition of CSC characteristics.

Maniotis et al[25] first described a new tumor vascular pattern, VM, which was totally diverse from existing tumor vascularization; in this pattern, tumor cells function as endothelial cells and form ECM-like vessels that allow blood flow in the circulating system. Vascular mimicry structures can interconnect with local blood vessels, thereby providing substantial blood nutrition for tumor tissues.[26] Multilineage differentiation plasticity is one of the characteristics of embryonic stem cells that is also evident during the development of VM. Normal tissue-resident stem cells could differentiate into endothelial cells and participate in normal tissue vascularization, which is called transdifferentiation. The transdifferentiative capacity and differentiation plasticity of normal stem cells are also common characteristics of CSCs.[27] In the statistical analysis we found that increased FZD2 expression was frequently observed in bigger tumors (diameter ≥5 cm), and in cell experiments that FZD2 played an essential role in the development of CSCs and the EMT phenotype of HCC cells. Therefore, we focused on VM formation to explore the further biological effect of FZD2-mediated EMT. Results of in vitro and in vivo experiments indicated that FZD2 could sufficiently promote VM formation. Hence, FZD2 could be considered as a new target treatment to suppress VM and metastasis of HCC.

The most exciting discovery in our study is the undescribed identification of certain signaling pathways linked to FZD2 dysregulation, including the Hippo pathway and pluripotency of stem cells pathway. Except for the CSCs feature discussed above, the link between FZD2 and the Hippo pathway is meaningful and warrants investigation. The Hippo pathway is a key regulator of organ size control and tissue homeostasis and frequently deregulated in many human cancers, including HCC.[28-31] When Hippo signaling is deregulated, its downstream regulators YAP enter the nucleus and increase transcriptional activation of genes involved in excessive cell proliferation and diminished apoptosis, ultimately leading to rapid progression of tumorigenesis. Activation of YAP in mouse liver leads to the development of HCC.[32,33] Knockout MST1/2, upstream inhibitors of YAP, in mouse liver also leads to the development of HCC.[34,35] Moreover, the Hippo pathway components also regulate other divergent physiological processes, including cell differentiation, stem cell self-renewal, reprogramming, and patterning.[6,29,36] Recent studies suggested that the canonical Wnt/β-Catenin pathway converged with the Hippo/YAP pathway to promote pluripotent stem cell features and tumorigenesis.[34,37-39] However, little attention was paid to the interaction between the noncanonical Wnt pathway and Hippo pathway. Here, we present pioneering research on a possible link between FZD2, a key transducer of the noncanonical Wnt pathway, and the Hippo-YAP pathway. FZD2 engendered activation of YAP and inhibition of upstream regulators, including MST1/2 and LATS. Based on this evidence, we believe our present study broadens the potential therapeutic target of the Hippo-YAP pathway to include FZD2 and sheds light on strategies for inhibiting this pathway for therapeutic benefit. However, additional studies are needed to confirm our hypothesis.

Taken together, our current study deepens our understanding of FZD2. First, FZD2 was found to be aberrantly upregulated in Chinese HCC patients with HBV infection. Second, by identifying numerous FZD2-regulated pathways and novel downstream targets, combined with functional studies, we robustly defined the oncogenic role of FZD2 in HCC. Third, we report for the first time that FZD2-induced EMT might promote VM and CSCs, and subsequently contribute to the progress and recurrence of HCC. Finally, this study revealed a promising correlation between the Hippo pathway and FZD2, thus establishing an extensive basis and providing a rationale for studying the role of FZD2 in HCC tumorigenesis.

ACKNOWLEDGMENTS

This work was supported by grants from Guangdong Provincial Science and Technology Projects (2017A020215132) and the National Natural Science Foundation of China (81872385).

CONFLICT OF INTEREST

Authors declare no conflicts of interest for this article.

ORCID

Dinghua Yang https://orcid.org/0000-0002-1442-5240

REFERENCES

1. Siegel RL, Miller KD, Jemal A. Cancer statistics, 2017. *CA Cancer J Clin*. 2017;67(1):7-30.
2. Forner A, Reig M, Bruix J. Hepatocellular carcinoma. *Lancet*. 2018;391(10127):1301-1314.
3. Steeg PS. Metastasis suppressors alter the signal transduction of cancer cells. *Nat Rev Cancer*. 2003;3(1):55-63.
4. Maluccio M, Covey A. Recent progress in understanding, diagnosing, and treating hepatocellular carcinoma. *CA Cancer J Clin*. 2012;62(6):394-399.
5. Willert K, Brown JD, Danenberg E, et al. Wnt proteins are lipid-modified and can act as stem cell growth factors. *Nature*. 2003;423(6938):448-452.
6. Deka J, Wiedemann N, Anderle P, et al. Bcl9/Bcl9l are critical for Wnt-mediated regulation of stem cell traits in colon epithelium and adenocarcinomas. *Cancer Res*. 2010;70(16):6619-6628.
7. Gupta S, Iljin K, Sara H, et al. FZD4 as a mediator of ERG oncogene-induced WNT signaling and epithelial-to-mesenchymal transition in human prostate cancer cells. *Cancer Res*. 2010;70(17):6735-6745.
8. Wu ZQ, Brabletz T, Fearon E, et al. Canonical Wnt suppressor, Axin2, promotes colon carcinoma oncogenic activity. *Proc Natl Acad Sci USA*. 2012;109(28):11312-11317.
9. Gujral TS, Chan M, Peshkin L, Sorger PK, Kirschner MW, MacBeath G. A noncanonical Frizzled2 pathway regulates epithelial-mesenchymal transition and metastasis. *Cell*. 2014;159(4):844-856.
10. Asano T, Yamada S, Fuchs BC, et al. Clinical implication of Frizzled 2 expression and its association with epithelial-to-mesenchymal transition in hepatocellular carcinoma. *Int J Oncol*. 2017;50(5):1647-1654.

11. Schnegg CI, Yang MH, Ghosh SK, Hsu MY. Induction of vasculogenic mimicry overrides VEGF-A silencing and enriches stem-like cancer cells in melanoma. *Cancer Res*. 2015;75(8):1682-1690.
12. Sun T, Zhao N, Zhao XL, et al. Expression and functional significance of Twist1 in hepatocellular carcinoma: its role in vasculogenic mimicry. *Hepatology*. 2010;51(2):545-556.
13. Zhang D, Sun B, Zhao X, et al. Twist1 expression induced by sunitinib accelerates tumor cell vasculogenic mimicry by increasing the population of CD133+ cells in triple-negative breast cancer. *Mol Cancer*. 2014;13:207.
14. Yang DH, Yoon JY, Lee SH, et al. Wnt5a is required for endothelial differentiation of embryonic stem cells and vascularization via pathways involving both Wnt/beta-catenin and protein kinase Calpha. *Circ Res*. 2009;104(3):372-379.
15. Qin L, Yin YT, Zheng FJ, et al. WNT5A promotes stemness characteristics in nasopharyngeal carcinoma cells leading to metastasis and tumorigenesis. *Oncotarget*. 2015;6(12):10239-10252.
16. Qi H, Sun B, Zhao X, et al. Wnt5a promotes vasculogenic mimicry and epithelial-mesenchymal transition via protein kinase Calpha in epithelial ovarian cancer. *Oncol Rep*. 2014;32(2):771-779.
17. Schmittgen TD, Livak KJ. Analyzing real-time PCR data by the comparative C(T) method. *Nat Protoc*. 2008;3(6):1101-1108.
18. Ou H, Liu X, Xiang L, Li X, Huang Y, Yang D. NVM-1 predicts prognosis and contributes to growth and metastasis in hepatocellular carcinoma. *Am J Cancer Res*. 2017;7(3):554-564.
19. Morel AP, Lievre M, Thomas C, Hinkal G, Ansieau S, Puisieux A. Generation of breast cancer stem cells through epithelial-mesenchymal transition. *PLoS ONE*. 2008;3(8):e2888.
20. Qiao L, Liang N, Zhang J, et al. Advanced research on vasculogenic mimicry in cancer. *J Cell Mol Med*. 2015;19(2):315-326.
21. Mani SA, Guo W, Liao MJ, et al. The epithelial-mesenchymal transition generates cells with properties of stem cells. *Cell*. 2008;133(4):704-715.
22. Santisteban M, Reiman JM, Asiedu MK, et al. Immune-induced epithelial to mesenchymal transition in vivo generates breast cancer stem cells. *Cancer Res*. 2009;69(7):2887-2895.
23. van der Horst G, van den Hoogen C, Buijs JT, et al. Targeting of alpha(v)-integrins in stem/progenitor cells and supportive microenvironment impairs bone metastasis in human prostate cancer. *Neoplasia*. 2011;13(6):516-525.
24. Zhu Z, Hao X, Yan M, et al. Cancer stem/progenitor cells are highly enriched in CD133+ CD44+ population in hepatocellular carcinoma. *Int J Cancer*. 2010;126(9):2067-2078.
25. Maniotis AJ, Folberg R, Hess A, et al. Vascular channel formation by human melanoma cells in vivo and in vitro: vasculogenic mimicry. *Am J Pathol*. 1999;155(3):739-752.
26. Forner A, Llovet JM, Bruix J. Hepatocellular carcinoma. *Lancet*. 2012;379(9822):1245-1255.
27. Yao XH, Ping YF, Bian XW. Contribution of cancer stem cells to tumor vasculogenic mimicry. *Protein Cell*. 2011;2(4):266-272.
28. Halder G, Johnson RL. Hippo signaling: growth control and beyond. *Development*. 2011;138(1):9-22.
29. Camargo FD, Gokhale S, Johnnidis JB, et al. YAP1 increases organ size and expands undifferentiated progenitor cells. *Curr Biol*. 2007;17(23):2054-2060.
30. Saucedo LJ, Edgar BA. Filling out the Hippo pathway. *Nat Rev Mol Cell Biol*. 2007;8(8):613-621.
31. Harvey KF, Zhang X, Thomas DM. The Hippo pathway and human cancer. *Nat Rev Cancer*. 2013;13(4):246-257.
32. Lee KP, Lee JH, Kim TS, et al. The Hippo-Salvador pathway restrains hepatic oval cell proliferation, liver size, and liver tumorigenesis. *Proc Natl Acad Sci USA*. 2010;107(18):8248-8253.
33. Nishioka N, Inoue K, Adachi K, et al. The Hippo signaling pathway components Lats and Yap pattern Tead4 activity to distinguish mouse trophectoderm from inner cell mass. *Dev Cell*. 2009;16(3):398-410.
34. Varelas X, Miller BW, Sopko R, et al. The Hippo pathway regulates Wnt/beta-catenin signaling. *Dev Cell*. 2010;18(4):579-591.
35. Zhou D, Conrad C, Xia F, et al. Mst1 and Mst2 maintain hepatocyte quiescence and suppress hepatocellular carcinoma development through inactivation of the Yap1 oncogene. *Cancer Cell*. 2009;16(5):425-438.
36. Hong JH, Hwang ES, McManus MT, et al. TAZ, a transcriptional modulator of mesenchymal stem cell differentiation. *Science*. 2005;309(5737):1074-1078.
37. Park HW, Kim YC, Yu B, et al. Alternative Wnt signaling activates YAP/TAZ. *Cell*. 2015;162(4):780-794.
38. Bejoy J, Song L, Zhou Y, Li Y. Wnt/Yes-associated protein interactions during neural tissue patterning of human induced pluripotent stem cells. *Tissue Eng Part A*. 2018;24(7–8):546-558.
39. Oudhoff MJ, Braam MJS, Freeman SA, et al. SETD7 controls intestinal regeneration and tumorigenesis by regulating Wnt/beta-catenin and hippo/YAP signaling. *Dev Cell*. 2016;37(1):47-57.

SUPPORTING INFORMATION

Additional supporting information may be found online in the Supporting Information section at the end of the article.

How to cite this article: Ou H, Chen Z, Xiang L, et al. Frizzled 2-induced epithelial-mesenchymal transition correlates with vasculogenic mimicry, stemness, and Hippo signaling in hepatocellular carcinoma. *Cancer Sci*. 2019;110:1169–1182. https://doi.org/10.1111/cas.13949